THE JOURNAL OF PHYSICAL CHEMISTRY A

ARTICLE

pubs.acs.org/JPCA

Kinetics Study of the Aromatic Bicyclic Peroxy Radical + NO Reaction: Overall Rate Constant and Nitrate Product Yield Measurements

Matthew J. Elrod*

Department of Chemistry and Biochemistry, Oberlin College, Oberlin, Ohio, 44074

ABSTRACT: The measurements of the overall bicyclic peroxy radical + NO rate constant for the 1,3,5-trimethylbenzene (1,3,5-TMB) system and of the nitrate product yields for the benzene, toluene, *p*-xylene, and 1,3,5-TMB systems were performed via the turbulent flow chemical ionization mass spectrometry technique. While the overall rate constant was found to be consistent with the value used in the most detailed aromatic oxidation kinetic model (Master Chemical Mechanism, MCM), the nitrate product yields were found to be generally lower than predicted by the MCM and to have a different aromatic species-specific dependence than the MCM predicts.

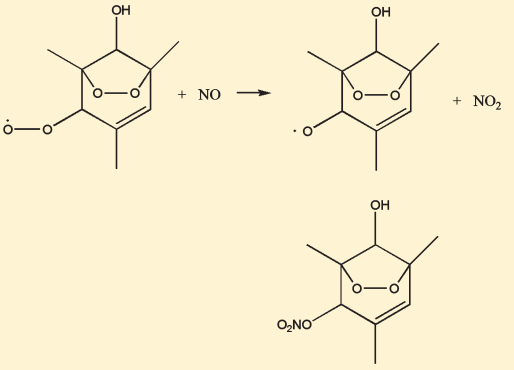

INTRODUCTION

Aromatic compounds are an important player in urban tropospheric ozone and secondary organic aerosol (SOA) pollution.[1,2] These species are introduced to the atmosphere largely from automobile exhaust, petroleum refining processes, and industrial solvent evaporation with benzene, toluene, the dimethylbenzenes (xylenes), ethylbenzene, and the trimethylbenzenes among the most atmospherically abundant compounds. It has been estimated that the aromatic class is responsible for up to 30% of the total nonmethane hydrocarbon (NMHC) content and up to 40% of the total OH reactivity in the Boston area.[3]

Like most NMHCs, aromatic compounds are believed to contribute to tropospheric ozone production via the reactions of peroxy radical (RO_2) intermediates with NO:

$$RO_2 + NO \rightarrow RO + NO_2 \quad (1a)$$

$$RO_2 + NO \rightarrow RONO_2 \quad (1b)$$

$$NO_2 + h\nu \rightarrow NO + O \quad (2)$$

$$O + O_2 + M \rightarrow O_3 + M \quad (3)$$

Note that eq 1a is a radical chain propagating step that leads to ozone production, while eq 1b is a radical chain terminating step that can suppress ozone production. The Master Chemical Mechanism (MCM) has been developed to provide an explicit representation of overall oxidation mechanism for aromatics, including kinetic models for the key ozone producing steps such as eq 1.[4] However, the MCM overpredicts ozone concentrations by 55% and underpredicts OH production by 44% in environmental chamber experiments meant to closely simulate atmospheric conditions for toluene oxidation.[4,5] The representation of eq 1 in the MCM is a potential source of error, as the MCM kinetic parameters are based on alkane peroxy radical analogues, rather than on actual measurements of the relevant aromatic peroxy radical rate constants. In particular, aromatic compound-specific overall rate constants (k_1) and nitrate product yield values (k_{1b}/k_1) are needed in order to ensure an accurate representation of the ozone producing potential of aromatic compounds. Interestingly, a recent study on urban air pollution in Mexico City suggested that if the k_{1b}/k_1 values for aromatic compounds were relatively large, the air quality policy of reducing aromatic emissions could actually lead to an increase in tropospheric ozone production (in part, because eq 1b leads to sequestering of NO, which leads to less ozone production by other NMHCs).[6]

In previous work, we investigated the products of the primary OH-initiated oxidation of many of the atmospherically abundant aromatic compounds using the turbulent flow chemical ionization mass spectrometry (TF-CIMS) technique under different oxygen, NO, and initial OH radical concentrations as well as a range of total pressures.[7,8] The bicyclic peroxy radical intermediate, the key peroxy radical believed to play a major role in ozone production by aromatics via eq 1, was detected for the first time. Based on product observations, we proposed a set of reactions for the bicyclic peroxy intermediate (given in Figure 1 for 1,3,5-trimethylbenzene—1,3,5-TMB—specifically). Figure 1 includes eq 1-type reactions, as well as reactions involving self-reactions of peroxy radicals. The self-reactions are proposed by analogy to the results obtained for the products formed from the self-reactions

Received: May 9, 2011
Revised: June 9, 2011
Published: June 10, 2011

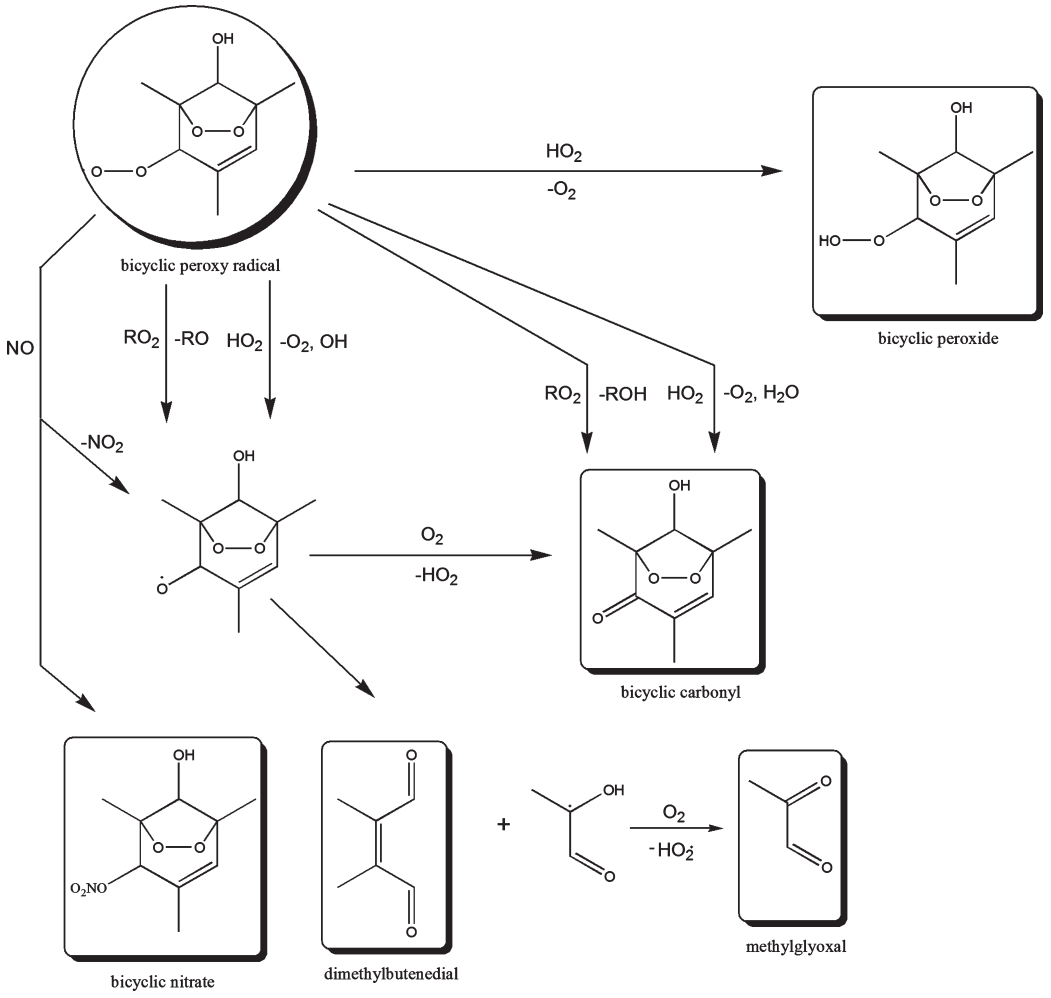

Figure 1. Bicyclic peroxy radical-dependent pathways in the primary OH-initiated oxidation of 1,3,5-trimethylbenzene (1,3,5-TMB).

of alkene-derived peroxy radicals[9]

$$RO_2 + R'O_2 \rightarrow RO + R'O + O_2 \quad (4a)$$
$$\rightarrow ROH + R'_{-H}O + O_2 \quad (4b)$$
$$\rightarrow R_{-H}O + R'OH + O_2 \quad (4c)$$

and from the reactions of acetyl peroxy radicals with hydroperoxy radical[10,11]

$$RO_2 + HO_2 \rightarrow ROOH + O_2 \quad (5a)$$
$$\rightarrow ROH + O_3 \quad (5b)$$
$$\rightarrow RO + OH + O_2 \quad (5c)$$

Our experiments suggested that the $RO_2 + HO_2$ reactions are the more important peroxy−peroxy reactions, and, owing to the relative high concentration of HO_2 as compared to RO_2 in the ambient atmosphere, it is much more likely that $RO_2 + HO_2$ reactions are more important in the actual atmosphere as well.

While we were able to detect nitrate products in our previous experiments, we were not able to quantify the nitrate product yield values. Previously, Wyche et al. had also reported the observation, but not quantitation, of nitrate products from the oxidation of 1,3,5-TMB.[12] Therefore, we suggested that it was important to measure the overall rate constants and product yield values for eqs 1 and 5 so as to better understand the competition between aromatic $RO_2 + NO$ and $RO_2 + HO_2$ processes in the atmosphere, and thus be able to better predict tropospheric ozone production from aromatic compounds.

This article describes the measurement of the overall bicyclic peroxy radical + NO rate constant for the 1,3,5-TMB system and of the nitrate product yields for the benzene, toluene, *p*-xylene, and 1,3,5-TMB systems via the turbulent flow chemical ionization mass spectrometry (TF-CIMS) technique. To the best of our knowledge, these studies constitute the first quantitative measurements of either kinetic parameter (k_1 and k_{1b}/k_1) for any aromatic system.

EXPERIMENTAL SECTION

Turbulent Fast Flow Tube. A schematic of the experimental apparatus is given in Figure 2 and is virtually identical to the method used in our previous aromatic oxidation product studies.[7,8] The main flow tube was 100 cm in length and constructed with 2.2 cm inner diameter Pyrex tubing. A large flow of oxygen carrier gas (30 STP L min^{-1}) was introduced at the rear of the flow tube to ensure turbulent flow conditions (Reynolds number ≈2100 for most experiments). The reactants necessary for the production of OH radicals were prepared in a 20 cm long, 1.25 cm inner diameter side arm. For the overall rate constant experiments, NO was added through the moveable injector, and an OH radical scavenger (propene) was introduced just downstream of the

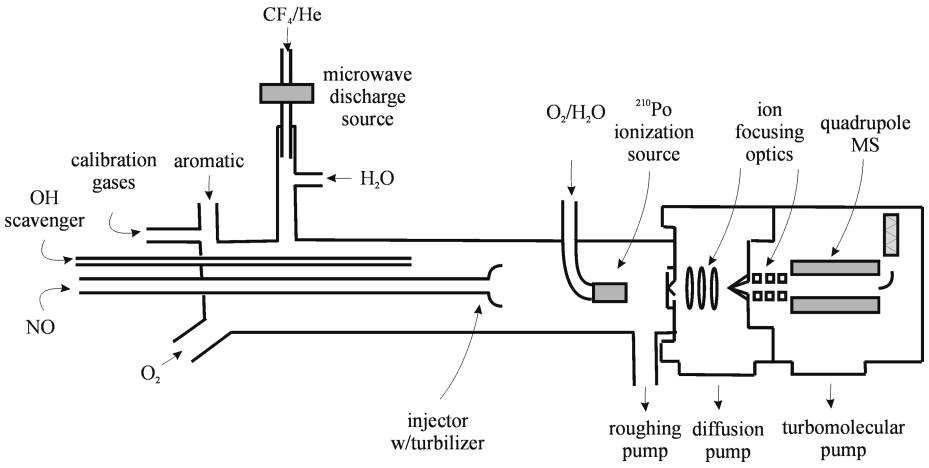

Figure 2. Experimental apparatus.

OH + aromatic reaction zone but upstream of the NO injection points. The injector encasement was made of corrugated Teflon tubing and allowed the injector to be moved to various injector positions ("time = zero" injector position is set just upstream of the ionization source) without breaking any vacuum seals. A fan-shaped Teflon device was placed at the end of the injector to enhance turbulent mixing. For the nitrate branching ratio experiments, NO was added to the rear of the flow tube in order to allow NO to immediately react with bicyclic peroxy radicals as they were formed in the OH + aromatic reaction zone. The calibration gases were also added to the rear of the flow tube. All gas flows were monitored with calibrated mass flow meters. A polonium-210 (^{210}Po) α-particle-emitting ionization source was placed between the flow tube and the entrance to the CIMS. Flow tube pressure and temperature were measured upstream of the ionization source. Pressure was measured using a 0−1000 torr capacitance manometer and was held at 200 torr for most of the experiments. At this pressure, the flow tube O_2 concentrations are identical to atmospheric O_2 concentrations (5×10^{18} molecules cm^{-3}). Temperature was determined using Cu-constantan thermocouples and was in the range 296−298 K for all experiments. Most of the flow tube gases were removed at the CIMS inlet using a 31 L s^{-1} roughing pump.

OH Source. The F + H_2O source utilizes the microwave discharge-initiated dissociation of CF_4, followed by reaction with H_2O:

$$CF_4 \rightarrow xF + CF_{4-x} \quad (6)$$

$$F + H_2O \rightarrow OH + HF \quad (7)$$

A dilute mixture of He/CF_4 was passed through a microwave discharge, produced by a Beenakker cavity operating at 50 W, to create fluorine atoms (eq 6). The dilute mixture was obtained by combining a 5.0 STP L min^{-1} flow of ultrahigh purity helium (99.999%) with a 1.0 STP mL min^{-1} flow of a 2.0% CF_4 (99.9%)/He mixture. The 5.0 STP L min^{-1} helium flow was first passed through a silica gel trap immersed in liquid nitrogen to remove any possible impurities. The fluorine atoms were then injected into the flow tube side arm and mixed with H_2O/He, produced by bubbling 5 mL min^{-1} He through a trap filled with H_2O to produce OH radicals (eq 7). Because H_2O is in great excess ([H_2O] ~ 2×10^{14} molecules cm^{-3}) and the F + H_2O reaction is very fast (1.4×10^{-11} cm^{-3} molecule^{-1} s^{-2}),[13] the OH-producing reaction has a very short lifetime of about 0.4 ms, thus ensuring that all F atoms are quickly consumed. This OH source was used in the present work (as opposed to the H + O_3 source used in our previous aromatic product studies) because of its ability to produce higher OH concentrations, which aided in the analytical detection of the low concentration bicyclic peroxy and nitrate species. Based on the measurement of the concentration of total products formed in the absence of NO, we estimate that the initial peroxy radical concentrations were equal to or less than 5×10^{11} molecules cm^{-3} for all systems.

Aromatic, OH Scavenger, and NO Concentrations. The benzene-d_6, toluene-d_3, *p*-xylene-d_{10}, and 1,3,5-trimethylbenzene systems were investigated. As discussed in our previous work,[7,8] the use of deuterated isotopes aids in the unique identification of the various product species (deuterated species are not available for 1,3,5-trimethylbenzene). The aromatic compounds were added to the rear of the flow tube as either gas mixtures (benzene and toluene) or by flowing He carrier gas through room temperature traps containing the liquid aromatic compounds (*p*-xylene, and 1,3,5-TMB). The aromatic concentrations were chosen such that the OH-aromatic lifetime[13] was about 5 ms, which is very short compared to the shortest flow tube residence times (~100 ms at 100 torr). For the nitrate branching ratio measurements, these conditions ensured that the dominant fate of OH was reaction with the aromatic compound. For the overall 1,3,5-TMB bicyclic peroxy radical + NO rate constant measurements, the presence of significant OH regeneration (which leads directly to bicyclic peroxy radical regeneration) required the use of an OH scavenger so that pseudo-first-order decay kinetics conditions could be achieved. Propene, which is known to efficiently form peroxy radicals in the presence of OH and O_2,[14] was introduced as a 20% propene/N_2 mixture through a special port downstream of the main OH + 1,3,5-TMB reaction zone but upstream of the NO injection points. Since our detection scheme is mass specific, the peroxy radicals generated due to the presence of the propene scavenger do not interfere with the 1,3,5-TMB bicyclic peroxy radical measurements. In order to ensure that the propene species outcompeted 1,3,5-TMB for OH under these conditions, the concentration of propene was chosen such that the OH-propene lifetime[13] was 10 times shorter than the OH-1,3,5-TMB lifetime. Because of the difficulty of the measurement, the overall 1,3,5-TMB bicyclic peroxy radical + NO rate constant measurements were carried out only at the ideal system operating

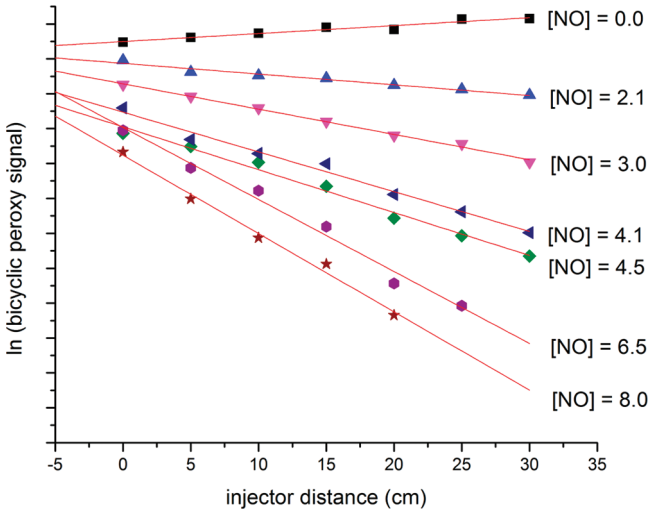

Figure 3. Pseudo-first-order 1,3,5-TMB bicyclic peroxy radical decay curves for the 1,3,5-TMB bicyclic peroxy radical + NO reaction at 100 torr, 297 K, 1110 cm/s velocity, and 2100 Reynolds number. NO concentrations are given in the units of 10^{12} molecules cm^{-3}.

pressure of 100 torr. For the overall rate constant measurements, NO was varied from 0 to 10 × 10^{12} molecules cm^{-3} and was held constant at 10 × 10^{12} molecules cm^{-3} for the nitrate branching ratio experiments (in order to drive the bicyclic peroxy + NO reaction quickly so that the bicyclic peroxy + NO reaction dominates over other potential reactions and relatively large nitrate concentrations were produced). In both cases, NO was introduced into the flow system as a 2% NO/N_2 mixture.

Pressure Dependence Studies. For the 1,3,5-TMB nitrate branching ratio measurements, the total pressure was varied from 100 to 400 torr by changing the roughing pump speed. While this variation also had the effect of changing the flow tube residence time by a linearly proportional amount, it did not change the relative rates of any of the processes, which are the relevant parameters in the analysis of the kinetics results.

CIMS Detection. The chemical ionization reagent ions were produced using a commercial polonium-210 α-particle emitting ionization source consisting of a hollow cylindrical (69 by 12.7 mm) aluminum body with 10 mCi (3.7 × 10^8 disintegrations s^{-1}) of polonium-210 coated on the interior walls. All oxygenated organic species were detected using a proton transfer (PTR-CIMS) scheme. The $H^+(H_2O)_n$ ions were produced by passing a large O_2 flow (7 STP L min^{-1}) through the ionization source with H_2O impurities being sufficiently abundant to produce an adequate amount of reagent ions. The dominant chemical reagent ion was $H^+(H_2O)_4$, and the predominant proton transfer species detected were the protonated (and partially hydrated) analogues of the neutral precursor oxygenated organic compounds. Ions were detected with a quadrupole mass spectrometer housed in a two-stage differentially pumped vacuum chamber. Flow tube gases (neutrals and ions) were drawn into the front chamber through a charged 0.1 mm aperture. The front chamber was pumped by a 6 in. 2400 L s^{-1} diffusion pump. The ions were focused by three lenses constructed from 3.8 cm inner diameter and 4.8 cm outer diameter aluminum gaskets and then entered the rear chamber through a skimmer cone with a charged 1.0 mm orifice. The skimmer cone was placed approximately 5 cm from the front aperture. The rear chamber was pumped by a 250 L s^{-1} turbomolecular pump. After the ions had passed

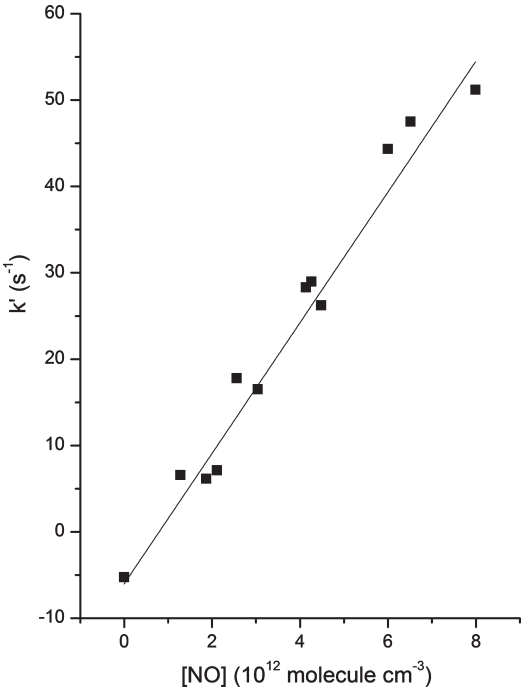

Figure 4. Determination of the overall bimolecular rate constant for the 1,3,5-TMB bicyclic peroxy radical + NO reaction from data in Figure 3.

through the skimmer cone, they were mass filtered and detected with a quadrupole mass spectrometer.

Nitrate Product Yield Studies. The nitrate product yield is defined as the flow tube concentration of the nitrate species divided by the sum of the flow tube concentrations of all measured products. Therefore, the nitrate product yield (defined as a percentage) is defined as follows:

$$\text{nitrate product yield } \% = \frac{[\text{nitrate}]}{\sum_j^n [\text{product}]_j} \times 100 \qquad (8)$$

This calculation requires the absolute concentration of each product. Calibration curves for authentic samples of the products benzaldehyde and *o*-cresol were constructed by flowing a known concentration of each substance into the flow tube and measuring the CIMS response. As extensively discussed in our earlier study on the toluene oxidation system,[15] because all other major products of the aromatic oxidation systems have either hydroxyl or carbonyl groups as the targets of the proton transfer CIMS reactions, it is reasonable to use the *o*-cresol or benzaldehyde (or the more convenient octanal) CIMS response factors, respectively, as proxy CIMS response factors for the calibration of species for which authentic samples are not available. However, because the nitrate group is also a potential proton transfer target, we also constructed a calibration curve for 3-nitrato-2-butanol, which we had previously used as a calibration standard for isoprene-derived hydroxynitrates,[16] in order to compare it to the *o*-cresol CIMS response factor. All m/z charge carriers with signals significantly above background were quantified (whether they could be definitively linked to a specific aromatic product species or not) so that the denominator in eq 8 could be determined as accurately as possible.

Table 1. Experimental and MCM-Predicted[4] Nitrate Yields

	pressure (torr)	exp. total nitrate yield (%)	exp. bicyclic yield (%)	exp. implied RO_2 + NO nitrate yield (%)	MCM RO_2 + NO nitrate yield (%)	MCM bicyclic yield (%)	MCM implied total nitrate yield (%)
benzene	200	3.4	38.1	8.9			
	760				8.2	35	2.9
toluene	200	2.9	52.8	5.5			
	760				11.1	65	7.2
p-xylene	200	2.5	76.6	3.3			
	760				13.8	62.5	8.6
1,3,5-TMB	100	2.8	95.0	2.9			
	200	3.1	95.1	3.3			
	400	2.1	96.5	2.2			
	760				15.7	79	12.4

RESULTS AND DISCUSSION

Overall Rate Constant Determination. Bimolecular rate constants were obtained via the usual pseudo-first-order approximation method, using NO as the excess reagent. Typical 1,3,5-TMB bicyclic peroxy radical decay curves as a function of injector distance are shown in Figure 3 for the NO kinetics measurements. The first-order rate constants obtained from fitting these decay curves (and additional ones not shown in Figure 3) were plotted against [NO], as shown in Figure 4. The small negative *y*-intercept evident in this figure is indicative of some peroxy radical loss on the injector, which is greatest at the shortest injector distances. The slope of the best fit line in Figure 4, 7.7 ± 0.7 $(2\sigma) \times 10^{-12}$ cm^3 molecule^{-1} s^{-1}, is equivalent to the bimolecular 1,3,5-TMB bicyclic peroxy radical + NO rate constant (k_1). As discussed above, errors in the apparent rate constants due to deviations from pseudo-first-order behavior resulting from OH regeneration are expected to be negligible under our conditions. The other likely systematic errors in the determination of rate constants are likely to occur in the measurements of gas flows, temperature, detector signal, and pressure. Considering such sources of error, it is estimated that rate constants can be determined with an accuracy of $\pm 30\%$ (2σ).

As discussed in the Introduction, the potential for bicyclic peroxy radicals to react either with other peroxy radicals (RO_2 or HO_2) or with NO is an important issue to understand since these processes may very well impact the interpretation of previous laboratory aromatic oxidation studies, as well as point to the potential for a more complicated NO-dependent atmospheric oxidation mechanism. It has been previously shown that the NO reaction rate constants for alkyl peroxy radicals (derived from alkane oxidation)[17] and alkyl hydroxyperoxy radicals (derived from alkene oxidation)[14] are largely invariant ($\sim 9.0 \times 10^{-12}$ cm^3 molecule^{-1} s^{-1}) for a number of different alkyl systems. Within the 2σ statistical uncertainty limit, the 1,3,5-TMB bicyclic peroxy radical + NO rate constant determined in the present work is identical to the previously determined alkyl peroxy + NO rate constants. This result validates the use of the value 9.0×10^{-12} cm^3 molecule^{-1} s^{-1} in the MCM for all aromatic bicyclic peroxy radical + NO rate constants.[4] Further, if $RO_2 + HO_2$ processes are indeed more important in aromatic oxidation systems than in alkane and alkene systems, then it appears that the rate constants must be larger for these reactions to explain the results, rather than the existence of a much smaller aromatic bicyclic peroxy + NO rate constant.

Nitrate Product Yields. As discussed in the Experimental section, because the bicyclic nitrate product has two potential proton transfer targets (the OH and ONO_2 groups), we carefully investigated the PTR-CIMS response factors for both *o*-cresol and 3-nitrato-2-butanol, two potential bicyclic nitrate calibration standards. We found that the PTR-CIMS response factor for 3-nitrato-2-butanol was a factor of 2 lower than for o-cresol. Previously, Wyche et al. reported some evidence for fragmentation of nitrates derived from the oxidation of 1,3,5-TMB using a H_3O^+-dominated PTR-CIMS method, as indicated by the observation of the NO_2^+ ion.[12] Since our measured PTR-CIMS response factor for 3-nitrato-2-butanol was lower than for *o*-cresol, fragmentation of the proton transfer nitrate product ion is a possible explanation for this result. However, we did not observe the NO_2^+ ion (nor any of its hydrates) in our system, nor did we observe any other species that would be consistent with fragmentation of the bicyclic nitrate ion species. Because we used a more hydrated chemical reagent ion ($H^+(H_2O)_4$) than did Wyche et al. (H_3O^+), a potential explanation for the difference in the fragmentation results is that our PTR-CIMS scheme is "softer" due to the ability of water molecules to carry away excess energy that might otherwise lead to fragmentation. In any case, because it is clear that PTR-CIMS response factors are usually more dependent on the functional group composition of the analytes than on the carbon backbone of the analytes,[18] we chose to use the 3-nitrato-2-butanol PTR-CIMS response to determine the bicyclic nitrate yields (via eq 8) in the present work. The nitrate product yield measurements are characterized by the same potential sources of systematic error as the overall rate constant measurements, as well as additional potential systematic error arising from the calibration process. Therefore, we estimate that the total measurement uncertainty to be on the order of 50%. In addition, the choice of the most appropriate PTR-CIMS response factor is a potential source of systematic error: if the *o*-cresol response factors were used instead, the bicyclic nitrate yields would be approximately a factor of 2 smaller.

The nitrate product yield results are presented in Table 1. In order to provide a more thorough interpretation of the results, as well as a detailed comparison to the predictions from the MCM,[4] several additional values are included in Table 1. Because we are able to identify and quantify the proportion of products that form through the bicyclic peroxy radical intermediate (as depicted in Figure 1), we can quantify the proportion of bicyclic peroxy radicals available for reaction with NO (listed in Table 1 as the experimental bicyclic yield). This value, combined with experimental total nitrate yield values, can be used to derive an experimentally implied RO_2 + NO nitrate yield (the fourth

column in Table 1), which is related to k_{1b}/k_1:

$$RO_2 + \text{NO nitrate yield } \% = \frac{[\text{nitrate}]}{\sum_j^n [\text{bicyclic pathway product}]_j} \times 100 = \frac{k_{1b}}{k_1} \times 100 \quad (9)$$

This is a useful quantity for comparison since all alkane and alkene species are thought to exclusively go through an RO_2 intermediate that is reactive with NO under atmospheric conditions, as opposed to the aromatic case where some final products are apparently formed without the formation of a "traditional" NO-reactive peroxy radical. This quantity can also be directly compared to the predictions of the MCM.

It is clear from Table 1 that the experimental results indicate that, over the range 100−400 torr, there is no discernible pressure dependence in the experimental total nitrate yields observed from the 1,3,5-TMB system. Therefore, it is reasonable to assume that these measurements for 1,3,5-TMB and the measurements made at 200 torr for the benzene, toluene, and *p*-xylene systems are applicable at the ambient atmospheric pressure of 760 torr. It is also clear that the experimental total nitrate yields are statistically identical across the four aromatic precursors. However, since the proportion of reactivity ascribed to the bicyclic peroxy radical intermediate increases with increasing methyl substitution on the aromatic ring, the experimentally implied RO_2 + NO nitrate yields are found to decrease with increasing methyl substitution (from 8.9% for benzene to about 3% for 1,3,5-TMB). On the other hand, the MCM predicts the reverse trend (from 8.2% for benzene to 15.7% for 1,3,5-TMB) for RO_2 + NO yields, as well increasing total nitrate yields as a function of methyl substitution of the aromatic ring. The MCM RO_2 + NO aromatic nitrate yields are largely based on extensive studies on the nitrate product yields for alkanes performed in the Atkinson lab.[19] These studies found that the nitrate yields increased as a function of increasing alkyl chain length, increasing pressure, and decreasing temperature, all of which suggest the importance of the rapid distribution of energy away from the nitrate-forming transition state. The present experimental results indicate that the dynamical nature of the RO_2 + NO nitrate reaction for aromatic systems is apparently quite different than that for alkane systems. In particular, it appears that methyl substitution actually disfavors the dynamical pathway to nitrate formation in aromatic systems. It is possible that the methyl groups do not provide an efficient means for the redistribution of energy in the energized transition state (as opposed to the apparent stabilizing effect of additional methylene groups in the alkane system case) and that they further disfavor the transition state perhaps through electronic and/or steric effects. In any case, it seems that alkane nitrate yield parameters used in the MCM are not appropriate for the aromatic oxidation system, and the total nitrate yields from aromatic systems are generally less than the MCM predicts.

CONCLUSION

The overall rate constant for the 1,3,5-TMB bicyclic peroxy radical + NO reaction was found to be, within statistical errors, identical to the generic RO_2 + NO rate constant derived from the alkane and alkene systems, and adopted in the MCM for all aromatic systems. However, the RO_2 + NO nitrate yields were found to decrease with increasing methyl substitution of the aromatic ring, a result that is the reverse of the MCM expectation (which was also based on alkane analogues). Therefore, it appears that the nitrate forming transition state for aromatic systems is dynamically different from the alkane systems, and nitrate products are formed less efficiently from aromatic precursors than the current MCM suggests.

AUTHOR INFORMATION

Corresponding Author
*E-mail: mjelrod@oberlin.edu.

ACKNOWLEDGMENT

This material is based upon work supported by the National Science Foundation under Grant No. 0753103.

REFERENCES

(1) Offenberg, J. H.; Lewis, C. W.; Lewandowski, M.; Jaoui, M.; Kleindienst, T. E.; Edney, E. O. *Environ. Sci. Technol.* **2007**, *41*, 3972.
(2) Velasco, E.; Lamb, B.; Westberg, H.; Allwine, E.; Sosa, G.; Arriaga-Colina, J. L.; Jobson, B. T.; Alexander, M. L.; Prazeller, P.; Knighton, W. B.; Rogers, T. M.; Grutter, M.; Herndon, S. C.; Kolb, C. E.; Zavala, M.; de Foy, B.; Volkamer, R.; Molina, L. T.; Molina, M. J. *J. Atmos. Chem. Phys.* **2007**, *7*, 329.
(3) *The mechanisms of atmospheric oxidation of aromatic hydrocarbons*; Calvert, J. G., Atkinson, R., Becker, K. H., Kamens, R. M., Seinfeld, J. H., Wallington, T. J., Yarwood, G., Eds.; Oxford University Press: Oxford, U.K., 2002.
(4) Bloss, C.; Wagner, V.; Jenkin, M. E.; Volkamer, R.; Bloss, W. J.; Lee, J. D.; Heard, D. E.; Wirtz, K.; Martin-Reviejo, M.; Rea, G.; Wenger, J. C.; Pilling, M. J. *Atmos. Chem. Phys.* **2005**, *5*, 641.
(5) Wagner, V.; Jenkin, M. E.; Saunders, S. M.; Stanton, J.; Wirtz, K.; Pilling, M. J. *Atmos. Chem. Phys.* **2003**, *3*, 89.
(6) Farmer, D. K.; Perring, A. E.; Wooldridge, P. J.; Blake, D. R.; Baker, A.; Meinardi, S.; Huey, L. G.; Tanner, D.; Vargas, O.; Cohen, R. C. *Atmos. Chem. Phys.* **2011**, *11*, 4085.
(7) Birdsall, A. W.; Andreoni, J. F.; Elrod, M. J. *J. Phys. Chem. A* **2010**, *114*, 10655.
(8) Birdsall, A. W.; Elrod, M. J. *J. Phys. Chem. A* **2011**, *115*, 5397.
(9) Jenkin, M. E.; Hayman, G. D. *J. Chem. Soc., Faraday Trans.* **1995**, *91*, 1911.
(10) Hasson, A. S.; Tyndall, G. S.; Orlando, J. J. *J. Phys. Chem. A* **2004**, *108*, 5979.
(11) Dillon, T. J.; Crowley, J. N. *Atmos. Chem. Phys.* **2008**, *8*, 4877.
(12) Wyche, K. P.; Monks, P. S.; Ellis, A. M.; Cordell, R. L.; Parker, A. E.; Whyte, C.; Metzger, A.; Dommen, J.; Duplissy, J.; Prevot, A. S. H.; Baltensperger, U.; Rickard, A. R.; Wulfert, F. *Atmos. Chem. Phys.* **2009**, *9*, 635.
(13) NIST, Chemical Kinetics Database, http://kinetics.nist.gov/kinetics/index.jsp, accessed 3/21/11.
(14) Miller, A. M.; Yeung, L. Y.; Kiep, A. C.; Elrod, M. J. *Phys. Chem. Chem. Phys.* **2004**, *6*, 3402.
(15) Baltaretu, C. O.; Lichtman, E. I.; Hadler, A. B.; Elrod, M. J. *J. Phys. Chem. A* **2009**, *113*, 221.
(16) Patchen, A. K.; Pennino, M. J.; Kiep, A. C.; Elrod, M. J. *Int. J. Chem. Kinet.* **2007**, *39*, 353.
(17) Eberhard, J.; Howard, C. J. *J. Phys. Chem.* **1997**, *101*, 3360.
(18) Zhao, J.; Zhang, R. *Atmos. Environ.* **2004**, *38*, 2177.
(19) Arey, J.; Aschmann, S. M.; Kwok, E. S. C.; Atkinson, R. *J. Phys. Chem. A* **2001**, *105*, 1020.